Genetics inMedicine | ARTICLE

Extrusion pump *ABCC1* was first linked with nonsyndromic hearing loss in humans by stepwise genetic analysis

Meng Li, MD[1,2], Lingyun Mei, PhD[1,2], Chufeng He, PhD[1,2], Hongsheng Chen, PhD[1,2], Xinzhang Cai, PhD[1,2], Yalan Liu, PhD[1,2], Runyi Tian, BS[3,4], Qi Tian, MD[3,4], Jian Song, PhD[1,2], Lu Jiang, PhD[1,2], Chang Liu, PhD[1,2], Hong Wu, PhD[1,2], Taoxi Li, BS[1,2,3], Jing Liu, MD[1,2], Ximan Li, MD[1], Yifang Yi, MD[1], Denise Yan, PhD[5], Susan H. Blanton, PhD[5,6], Zhengmao Hu, PhD[3,4], Xuezhong Liu, MD[1,5,6], Jiada Li, PhD[3,4,7], Jie Ling, PhD[1,8] and Yong Feng, PhD[1,2,9,10]

Purpose: To determine the genetic etiology of deafness in a family (HN-SD01) with autosomal dominant nonsyndromic hearing loss (NSHL).

Methods: Stepwise genetic analysis was performed on family HN-SD01, including hotspot variant screening, exome sequencing, virtual hearing loss gene panel, and genome-wide linkage analysis. Targeted region sequencing was used to screen *ABCC1* in additional cases. Cochlear expression of *Abcc1* was evaluated by messenger RNA (mRNA) and protein levels. Computational prediction, immunofluorescence, real-time quantitative polymerase chain reaction, and flow cytometry were conducted to uncover functional consequences of candidate variants.

Results: Stepwise genetic analysis identified a heterozygous missense variant, *ABCC1*:c.1769A>G (p.Asn590Ser), cosegregating with phenotype in HN-SD01. Screening of *ABCC1* in an additional 217 cases identified candidate pathogenic variants c.692G>A (p.Gly231Asp) in a sporadic case and c.887A>T (p.Glu296Val) in a familial proband. *Abcc1* expressed in stria vascularis and auditory nerve of mouse cochlea. Immunofluorescence showed p.Asn590Ser distributed in cytomembrane and cytoplasm, while wild type was shown only in cytomembrane. Besides, it generated unstable mRNA and decreased efflux capacity of ABCC1.

Conclusion: Stepwise genetic analysis is efficient to analyze the genetic etiology of NSHL. Variants in *ABCC1* are linked with NSHL and suggest an important role of extruding pumps in maintaining cochlea function.

Genetics in Medicine (2019) 21:2744–2754; https://doi.org/10.1038/s41436-019-0594-y

Keywords: hearing loss; stepwise genetic analysis; *ABCC1*; extrusion pump; cochlea

INTRODUCTION

Hearing impairment is the most common sensory deficit, with an incidence of 1 in 500 individuals worldwide.[1] Approximately 50% of hearing loss has a genetic basis, and approximately 70% of these cases are classified as nonsyndromic hearing loss (NSHL) due to the absence of additional clinical manifestations. Autosomal dominant nonsyndromic hearing loss (ADNSHL) comprises ~20% of cases with hereditary hearing loss, characterized by postlingual progressive hearing loss initially affecting high frequencies.[2,3] Currently, 60 ADNSHL loci have been mapped, and 38 causative genes have been identified (http://hereditaryhearingloss.org/). With the rapid development of massively parallel sequencing technology, the pace of gene discovery has been accelerated.

ATP-Binding Cassette Subfamily C1 (*ABCC1*) lies on chromosome 16p13.11 and encodes multidrug resistance–associated protein 1 (MRP1). It was originally discovered in lung cancer cells as a cause of drug resistance for efflux of multiple anticancer drugs.[4] Now it has been found that *ABCC1* has a ubiquitous tissue distribution[5] and mediates a protective role in multiple organs through excretion of toxic compounds and their metabolites. *Abcc1*(-/-) mice

[1]Department of Otolaryngology, Xiangya Hospital, Central South University, Changsha, Hunan, China; [2]Key Laboratory of Otolaryngology Major Diseases Research of Hunan Province, Changsha, Hunan, China; [3]Center for Medical Genetics, School of Life Sciences, Central South University, Changsha, Hunan, China; [4]Hunan Key Laboratory of Medical Genetics, Changsha, Hunan, China; [5]Department of Otolaryngology, University of Miami Miller School of Medicine, Miami, FL, USA; [6]Dr. John T. Macdonald Foundation Department of Human Genetics, University of Miami Miller School of Medicine, Miami, FL, USA; [7]Hunan Key Laboratory of Animal Models for Human Diseases, Changsha, Hunan, China; [8]Institute of Molecular Precision Medicine, Xiangya Hospital, Central South University and Hunan Key Laboratory of Molecular Precision Medicine, Changsha, Hunan, China; [9]National Clinical Research Center for Geriatric Disorders, Xiangya Hospital, Central South University, Changsha, Hunan, China; [10]Hunan Jiahui Genetics Hospital, Changsha, Hunan, China. Correspondence: Jie Ling (lingjie@sklmg.edu.cn) or Yong Feng (fengyong_hn@hotmail.com)
These authors contributed equally: Meng Li, Lingyun Mei
These authors contributed equally: Yong Feng, Jie Ling

Submitted 19 March 2019; accepted: 17 June 2019
Published online: 5 July 2019

exhibit an increase in the levels of glutathione (GSH) in most tissues and are more sensitive to xenobiotics.[6] Variants of *ABCC1* are associated with cancer patients' susceptibility to doxorubicin-induced cardiotoxicity[7] and age-related macular degeneration.[8]

So far, no report has linked extrusion pump *ABCC1* with hearing loss in humans. In this study, we identified a heterozygous missense variant in *ABCC1* that was associated with ADNSHL in a large Chinese Han family.

MATERIALS AND METHODS

Patients and clinical examinations

We recruited a five-generation Chinese Han family (HN-SD01) from Hunan Province, China, with postlingual ADNSHL. Twenty-eight members (10 affected) participated in this study and each signed informed consent. All subjects underwent detailed clinical history interviews and physical examinations to rule out environmental factors causing hearing impairment and the presence of a syndrome. Hearing levels were measured by pure tone audiometry. For the proband, additional auditory evaluations were performed including distortion product otoacoustic emission (DPOAE), auditory brainstem response (ABR), auditory steady-state response (ASSR), and temporal bone high-resolution computed tomography scanning (HRCT). Genomic DNA was extracted from peripheral blood samples following standard phenol-chloroform methods. We also recruited additional 217 familial probands or sporadic cases with postlingual NSHL for variant screening of the candidate gene. Common variants of *GJB2* or *SLC26A4* and mitochondrial 12S ribosomal RNA (rRNA) were previously excluded in these 217 affected cases. This study was approved by the ethics committee of Xiangya Hospital, Central South University.

Gene microarray detection of hotspot variant

DNA from proband IV12 was tested by a gene microarray in the Ear, Nose, and Throat Department of Xiangya Hospital, using multiplex polymerase chain reaction (PCR) coupled with dual-color arrayed primer extension. This microarray includes ten Chinese hotspot variants for hearing loss,[9] including *GJB2* (NM_004004.5:c.512_513insAAGG, NM_004004.5:c.176_191del, NM_004004.5:c.235delC, NM_004004.5:c.299_300delAT),[10] *SLC26A4* (NM_000441.1:c.2168A>G, NM_000441.1:c.919-2A>G, NM_000441.1:c.1174A>T, NM_000441.1:c.1229C>T),[11,12] and mitochondrial 12S rRNA (NC_012920.1:m.1555A>G, NC_012920.1:m.1494C>T).[13]

Exome sequencing

Exome sequencing (ES) was conducted in two affected (IV5, IV12) members and one unaffected (IV10) member, following the manufacturer's instructions. Briefly, genomic DNA was fragmented and 180–280 base pair products were selected. Exons and flanking intronic regions were captured by Agilent SureSelect Human All Exon V6 enrichment platform (Agilent Technologies, Santa Clara, CA), and then sequenced on Illumina HiSeq 4000 platform (Illumina, San Diego, CA) with an average sequencing depth of 50×.

Establishment of virtual hearing loss gene panel

A virtual hearing loss gene panel is an ES-based disease-associated bioinformatic analysis strategy. It contains known hearing loss genes (http://hereditaryhearingloss.org/) and genes of syndromic disorders including hearing loss as a significant finding (https://www.ncbi.nlm.nih.gov/clinvar/) (Supplementary Table S1). This virtual gene panel can narrow the scope of candidate pathogenic variants from the massive data of ES.

Disease-associated bioinformatic and cosegregation analysis

Original image files of the exome sequencing were created with the Illumina pipeline. Clean data were then aligned to human reference genome hg19 (University of California–Santa Cruz [UCSC] version) using the Burrows–Wheeler alignment tool. Duplicate reads were detected by Picard 1.14 (http://broadinstitute.github.io/picard/). CNVnator v0.2.2 software was used to detect copy-number variants (CNVs). Single-nucleotide variants (SNVs) and indels were identified using Genome Analysis Toolkit (GATK) Unified Genotyper in parallel with the SAMtools pipeline. First, we determined whether variants detected in our study have been reported as high-frequency pathogenic variants of known hearing loss genes such as *GJB2* and *SLC26A4*.[14] Variants were further annotated based on their presence and pathogenicity information in ClinVar (https://www.ncbi.nlm.nih.gov/clinvar/) and the Human Gene Mutation Database (HGMD) (www.hgmd.cf.ac.uk/) for identification of variants already associated with hearing loss. Subsequently, variants were filtered as nonsynonymous, from protein coding or splicing sites, followed with minor allele frequency (MAF) ≤0.01 in public databases (1000 Genomes, Exome Variant Server, Genome Aggregation Database [gnomAD], HGMD, and dbSNP).

Disease-associated bioinformatic analysis was first implemented on known hearing loss genes. Candidate variants were extracted from the massive amount of ES data by virtual hearing loss gene panel. This process was easily achieved using the VLOOKUP function in Microsoft Excel. Further screening for undiscovered hearing loss genes was performed by genome-wide linkage analysis, described in the following section.

Primers were designed to amplify gene segments including variants using Primer3 (http://primer3.ut.ee). Sanger sequencing of PCR products was conducted in all family members for cosegregation analysis.

Genome-wide linkage analysis

Eighteen family members were subjected to genome-wide linkage analysis using OmniZhongHua-8 v1.3 BeadChip (Illumina) containing 878,291 single-nucleotide polymorphism (SNP) markers. Genotype calling and quality control were

processed with Illumina GenomeStudio Genotyping Module. SNPs with Mendelian errors or call rates lower than 100% were removed. In total, 11,265 tag SNPs, about 0.3 cM per genomic region, were subjected to parametric linkage analysis with Merlin v.1.1.2 to calculate the logarithm of the odds (LOD) scores. The inheritance model was considered as a complete penetrance autosomal dominant model with a rare disease allele frequency of 0.0001.

Candidate pathogenic variants were obtained by mapping filtered variants acquired from exome sequencing to the

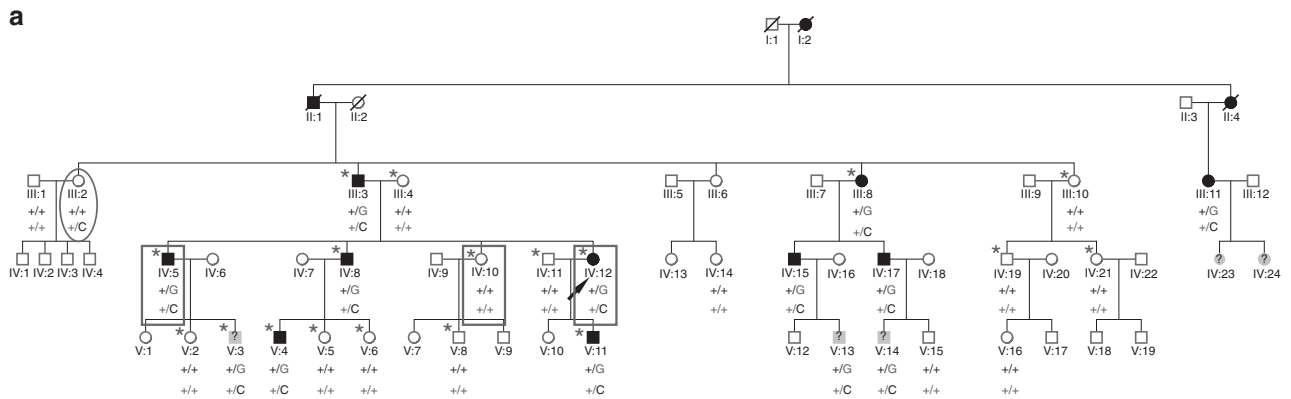

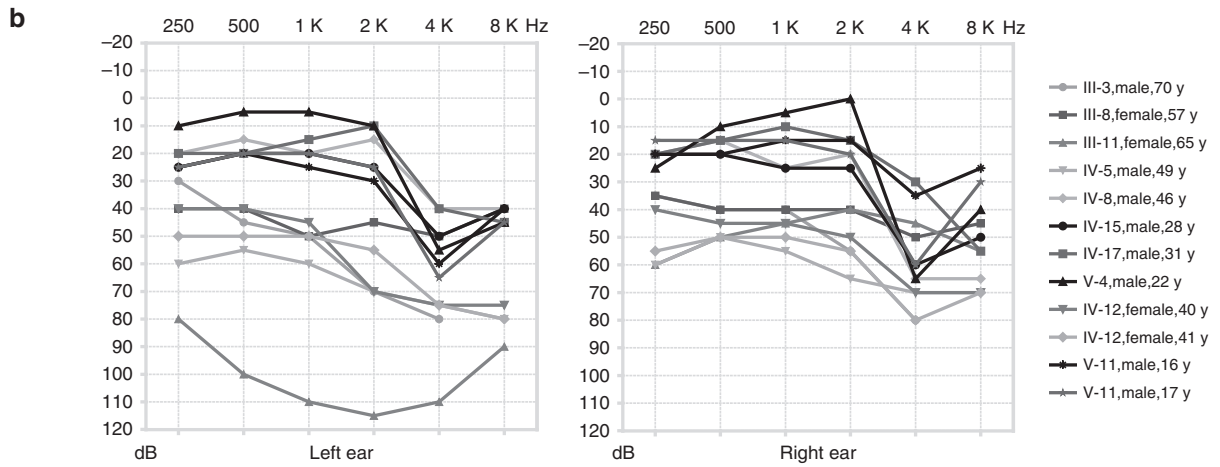

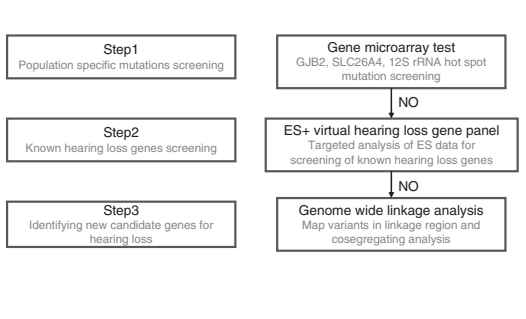

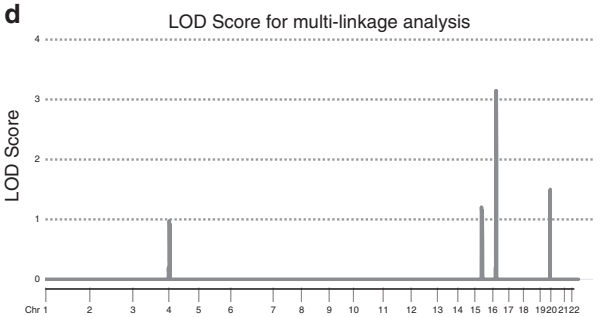

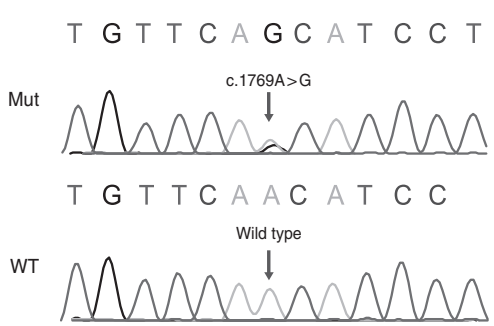

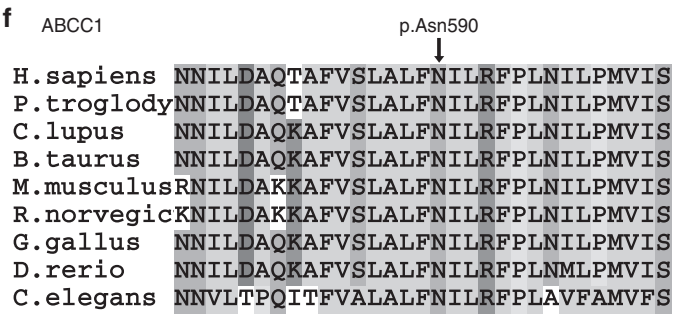

linkage area. Variants cosegregating with hearing loss in HN-SD01 were retained. Sanger sequencing was used to screen 281 Han control individuals with normal hearing.

Mutation screening

Targeted region sequencing was selected as an efficient and cost-effective way to uncover possible variants in additional 217 patients with postlingual hearing loss. Multiplex PCR primers were designed to capture all 31 exons and flanking sites of *ABCC1* (http://www.igenetech.com/design). Amplified enriched DNA was subjected to next-generation sequencing (NGS) on a HiSeq system (Illumina). Data processing methods were similar to those used in exome sequencing (described above). High-frequency variants (MAF >0.001) and variants predicted to be benign by computational tools including MutationTaster, PROVEAN, and SIFT were excluded. Filtered candidate variants were subsequently confirmed by Sanger sequencing.

Model building and structural analysis

Three-dimensional (3D) modeling of ABCC1 and variants were performed using I-TASSER (http://zhanglab.ccmb.med.umich.edu/I-TASSER) with structures of bovine multidrug resistance protein 1 (MRP1) (PDBID: 5UJ9) as templates. Wild-type (WT) and variant protein structures of ABCC1 were visualized and manipulated using PyMol (DeLano Scientific, Palo Alto, CA).

Expression of *Abcc1* in mouse inner ear

Total RNA was isolated from postnatal day 3–4 (P3–4) C57BL/6 mice inner ears and was reverse transcribed to complementary DNA (cDNA) with the RevertAid™ First Strand cDNA Synthesis Kit (Thermo Scientific). Fragments of exons 4–5 (134 bp), 21–22 (97 bp), and 30–31 (124 bp) were amplified using three primer pairs designed by Primer3 (http://primer3.ut.ee). Western blot analysis was conducted on P3–4 mice cochlea and compared with lung and kidney tissues. Immunofluorescence staining of Abcc1 was performed on frozen sections from P28 mice cochlea (detailed protocols are shown in Supplementary Methods).

Mutagenesis and subcellular location analysis of *ABCC1*-WT and *ABCC1*-A1769G

The *ABCC1*-A1769G variant was generated by the Nanjing GenScript Biotechnology Company (Nanjing, China) with site-directed mutagenesis, using a pcDNA3.1-C-(K)DYK-h*ABCC1*-WT construct tagged with a C-terminal flag as a template. All plasmids were validated by Sanger sequencing of the *ABCC1* insert. HEK293 cells were seeded on gelatinized coverslips in a 6-well plate (0.5×10^6 cells per well), and transfected with pcDNA3.1-C-(K)DYK expression vectors containing WT or variant cDNA using Lipofectamine 2000 (Invitrogen) 24 hours later, according to manufacturer's instructions. Immunofluorescence was performed 36–48 hours after transfection as previously described[15] (details are shown in Supplementary Methods).

Expression and functional analysis of *ABCC1* in lymphoblastoid cell lines from patients and normal controls

Lymphocytes were isolated from the peripheral blood of two affected and two unaffected individuals in family HN-SD01 and transfected by Epstein–Barr virus to establish immortalized lymphoblastoid cell lines. Total RNA was extracted from these cell lines using TRIzol (Invitrogen) and was reverse transcribed (RT) to cDNA as described above. Primers were designed to amplify exons 12–14. Sanger sequencing of RT-PCR products was used to test whether or not the variant was transcribed to messenger RNA (mRNA). Real-time quantitative PCR (RT-qPCR) was performed to compare mRNA levels between the affected and unaffected lymphoblastoid cell lines. The relative standard curve method was used to analyze target gene with Maxima™ SYBR Green/ROX qPCR Master Mix Kit (Fermentas). Expression was normalized to *GAPDH* in the same sample and was measured by three independent experiments. Reactions were run on Bio-Rad CFX96 Touch Deep Well Real-Time PCR Detection System. All primer pairs for RT-qPCR and RT-PCR are listed in Supplementary Table S2. To determine the functional consequence of p.Asn590Ser, we examined the export of 5-carboxyseminaptharhodafluor (SNARF-1), an MRP1 specific substrate.[16,17] Details of the SNARF-1 efflux assay are presented in Supplementary Methods.

RESULTS

Clinical characterizations of the five-generation ADNSHL family

We ascertained a pedigree of Chinese Han origin, HN-SD01, with bilateral, postlingual, mild-to-severe ADNSHL, without tinnitus or vestibular symptoms (Fig. 1). In most affected individuals, hearing loss started with high-frequency loss at the second or third decade, and subsequently worsened in all frequencies at the fourth or fifth decade. Individual III:11 exhibited asymmetric hearing loss due to sudden hearing loss in the left ear in the third decade. The youngest affected

Fig. 1 Pedigree, audiograms, and stepwise genetic analysis of family HN-SD01. (**a**) Individuals selected for linkage analysis and exome sequencing are marked with asterisks and red rectangles, respectively. Black and white symbols each represent affected and normal individuals. Gray symbols with question mark indicate individuals with uncertain phenotypes. Proband IV:12 is indicated by an arrow. "+" indicates the reference allele. Genotypes of the two candidate variants (C denotes NM_001184998.1:c.3122T>C in *KIAA0430*; G denotes NM_004996.3:c.1769A>G in *ABCC1*) are shown for all family members. Individual III:2 (73 years old), highlighted by the red oval, harbors a key recombination event. (**b**) Audiograms of the affected individuals in family HN-SD01. Individuals IV:12 and V:11 were followed up for two years. (**c**) Stepwise genetic analysis strategy. (**d**) Multipoint parametric linkage analysis demonstrated a linkage interval with maximum logarithm of the odds (LOD) scores of 3.149 in chromosome 16. (**e**) Sequence analyses of wild type and variant identified in family HN-SD01. (**f**) Asn590 of ABCC1 is highly conserved through evolution. *ES* exome sequencing, *rRNA* ribosomal RNA, *WT* wild type.

individual, V:11, was diagnosed with symmetric high-frequency hearing loss at the age of 17, with an initial hearing loss in the left ear at the age of 16. Clinical examinations including otoscopy, ABR, ASSR, DPOAE, and temporal bone HRCT for the proband were negative, excluding auditory neuropathy spectrum disorders and inner ear malformations. There was no excessive noise exposure, special medication history, or complaints of other systemic abnormalities, thus

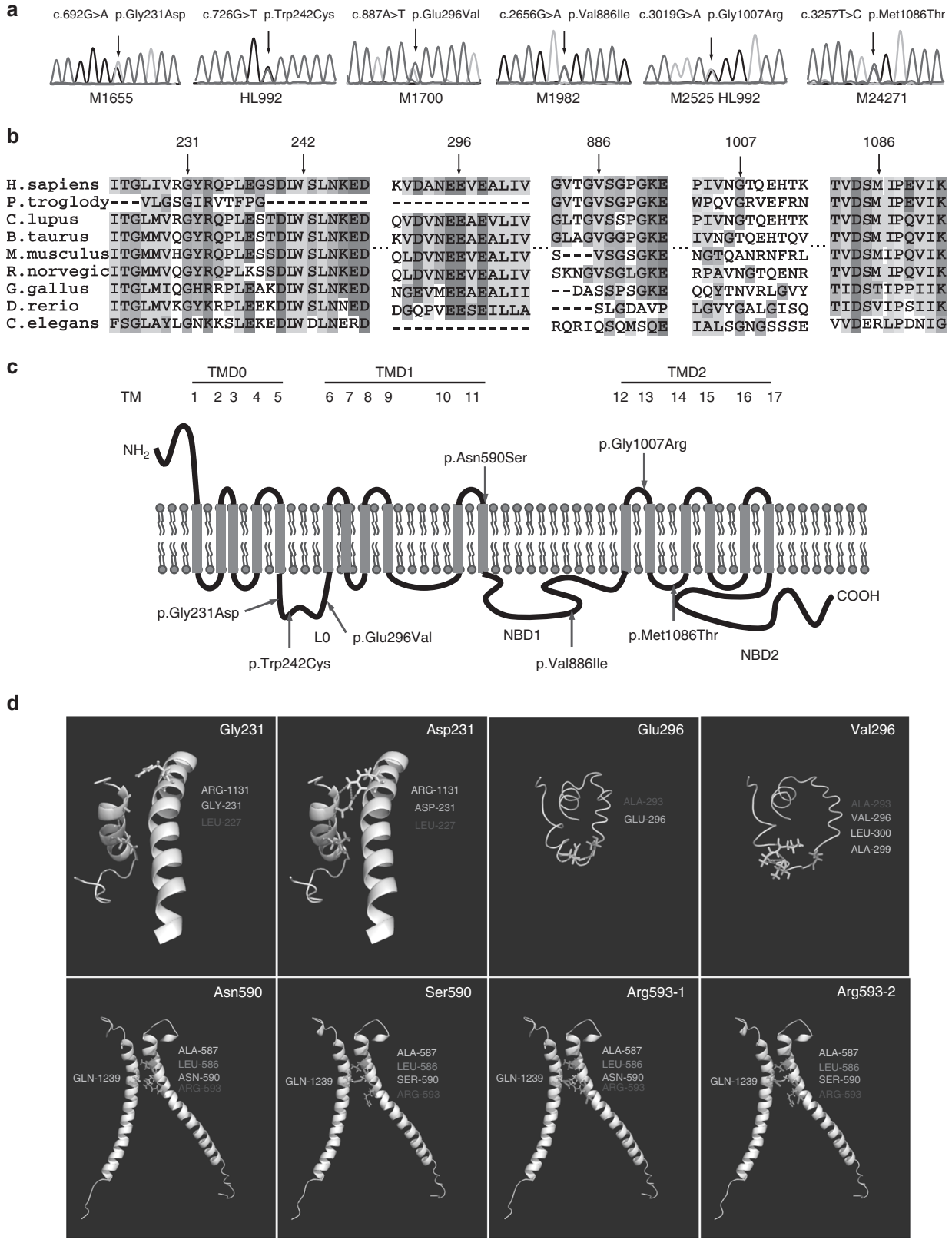

ruling out a syndromic form of hearing loss. During our nearly two years of clinical follow-up, the pure tone threshold of family member IV:12 was found to be increased by nearly 10 dB.

Genetic analysis of HN-SD01

Stepwise strategies were performed to identify the genetic etiology of hearing loss in family HN-SD01. Initial screening of *GJB2*, *SLC26A4*, and mitochondrial 12S rRNA in proband IV:12 was negative and thus eliminated common hearing loss genes in this family (Fig. **1c**).

Subsequently, ES was conducted in two affected and one unaffected siblings (Fig. **1a**). The average sequencing depth was 50× and minimum coverage for targeted region by 10× was 97.9%. CNVs identified in the two affected siblings (IV:12 and IV:5) were not associated with known hearing loss genes. No high-frequency variants in known hearing loss genes were detected in our data. A total of 905 variants in coding and splicing sites with MAF ≤ 0.01 were retained from the 19,185 identified variants. A virtual hearing loss gene panel for known hearing loss genes was constructed, and 13 candidate variants were extracted. However, none of these variants segregated with the phenotype, indicating a novel gene was responsible for hearing loss in HN-SD01.

For further identification of pathogenic variants, multipoint genome-wide linkage analysis was carried out on seven affected, ten unaffected, and one uncertain phenotype members of pedigree HN-SD01 (Fig. **1a**). The result identified an 8.15-Mb candidate region on chromosome 16p13.3-16p12.3 with a maximum multipoint parametric LOD score of 3.149 (Fig. **1d**). Mapping filtered data from the ES to the positional linkage interval revealed only two variants: *KIAA0430* (NM_001184998.1:c.3122T>C, NP_001171927.1:p.[Val1041Ala]) and *ABCC1* (NM_004996.3:c.1769A>G, NP_004987.2:p.[Asn590Ser]) (Fig. **1a**). Variant *KIAA0430* (NM_001184998.1:c.3122T>C)(*KIAA0430* c.3122T>C) was present in normal hearing sibling III:2 (73 years old when recruited), and was predicted to be nonpathogenic (SIFT, PolyPhen-2, PROVEAN, LRT, and Combined Annotation Dependent Depletion [CADD]).[18] *ABCC1* (NM_004996.3:c.1769A>G) (*ABCC1* c.1769A>G) was validated as the sole variant segregating with hearing loss in all family members (Fig. **1a, e**). It has a highest subpopulation frequency of 0.0001198 (3 in 25,034 alleles) in Europeans, 0.00005118 (1 in 19,538 alleles) in East Asians, and total of 0.00003559 (10 in 280,968 alleles) in the Genome Aggregation Database (gnomAD). It was also not present among 564 ethnically matched chromosomes from controls with normal hearing. Variant p.Asn590Ser is predicted to be deleterious or possibly damaging by SIFT, PolyPhen-2, PROVEAN, LRT, CADD, and MutationTaster and is highly conserved throughout evolution (Fig. **1f**).

Screening of *ABCC1* detected new variants in sporadic or familial cases

To identify evidence to support our findings, we subsequently sequenced all exons and exon–intron boundaries of *ABCC1* in an additional 217 subjects with postlingual NSHL. Age at onset of hearing loss varied from the first to the fourth decade. Pure tone audiometry indicated sensorineural hearing loss, and severity varied from mild to profound. Six variants in *ABCC1* were identified in seven subjects, with one individual having two different variants (HL992) (Fig. **2a**, Table **1**). The variant NM_004996.3:c.3019G>A, NP_004987.2:p.(Gly1007Arg) (c.3019G>A, p.Gly1007Arg) was present in two sporadic cases (M2525, HL992), but has a MAF of 0.0043 in ethnically matched controls in gnomAD, and is thus considered as a polymorphism. Variant NM_004996.3:c.726G>T, NP_004987.2:p.(Trp242Cys) (c.726G>T, p.Trp242Cys) occurred in one sporadic case (HL992) and was also classified as a polymorphism based on MAF >0.001 reported in ethnically matched controls in gnomAD. Variants NM_004996.3:c.2656G>A, NP_004987.2:p.(Val886Ile) (c.2656G>A, p.Val886Ile) and NM_004996.3:c.3257T>C, NP_004987.2:p.(Met1086Thr) (c.3257T>C, p.Met1086Thr) were each identified in one sporadic case (M1982, M24271). These variants were not conserved through evolution (Fig. **2b**) and were predicted to be benign or tolerable, and were thus considered as polymorphisms. Variants NM_004996.3:c.692G>A, NP_004987.2:p.(Gly231Asp) (c.692G>A, p.Gly231Asp) and NM_004996.3: c.887A>T, NP_004987.2:p.(Glu296Val) (c.887A>T, p.Glu296Val) were identified in a sporadic case (M1655) and in a familial proband (M1700), respectively. Both variants were absent in gnomAD and the Exome Aggregation Consortium (ExAC) database. Functional prediction and conservation analyses suggested that both missense variants (p.Gly231Asp and p.Glu296Val) are deleterious or possibly damaging, and are highly conserved throughout evolution (Fig. **2b**, Table **1**). However, no other family members were recruited for further cosegregation analysis. In addition, the variant c.1769A>G (p.Asn590Ser) was not detected in these cases.

Three-dimensional modeling of human ABCC1

Gly231 and Glu296 residues are located in domain L0 (Fig. **2c**). Variant p.Gly231Asp changes hydrogen bonds between L0 and TM15 (Fig. **2d**), and variant p.Glu296Val alters hydrogen bonds in adjacent amino acids, and both may

Fig. 2 *ABCC1* variants identified in postlingual hearing loss cases. (**a**) Sequence analysis for six variants screened in familial and sporadic cases. (**b**) Conservation analysis of amino acid sequences was performed by ClustalX Multiple Sequence Alignment tool. Variants at position 231, 242, 296 were conserved through evolution. (**c**) Predicted topology of ABCC1 secondary structure. ABCC1 contains five domain structures with two nucleotide binding domains (NBDs) and 17 transmembrane helices (TMs) in three transmembrane domains (TMD0, TMD1, and TMD2). Linker L0 at COOH-terminus connects TMD0 and TMD1. Locations of variants identified in familial and sporadic cases are marked by red arrows. (**d**) Three-dimensional modeling of human ABCC1.

Table 1 Variants of *ABCC1* identified in familial or sporadic cases with postlingual hearing loss

ID	F/S	OA	HL degree	NT change	AA change	MAF[a]	SIFT	PolyPhen-2	LRT	MutationTaster	GERP	phylop
HL992	S	16	Profound	c.3019G>A	p. Gly1007Arg	0.004350 (EA)	Damaging	PD	D	Disease causing	C	C
HL992	S	16	Profound	c.726G>T	p.Trp242Cys	0.001076 (EA)	Damaging	PD	D	Disease causing	C	C
M1655	S	22	Moderate	c.692G>A	p.Gly231Asp	–	Damaging	PD	D	Disease causing	C	C
M1700	F	14	Severe	c.887A>T	p.Glu296Val	–	Damaging	PD	D	Disease causing	C	C
M1982	S	17	MS	c.2656G>A	p.Val886Ile	0.0004837 (other)	Tolerable	Benign	N	Polymorphism	NC	NC
M24271	S	18	MS	c.3257T>C	p.Met1086Thr	0.0002560 (EA)	Tolerable	Benign	D	Polymorphism	C	C
M2525	S	21	Moderate	c.3019G>A	p. Gly1007Arg	0.004350 (EA)	Damaging	PD	D	Disease causing	C	C

RefSeq: NM_004996.3 for coding DNA reference sequence; NP_004987.2 for protein reference sequence.
AA amino acid, *C* conserved, *D* deleterious, *EA* East Asian, *F* familial, *HL* hearing loss, *MAF* minor allele frequency, *MS* moderate to severe, *N* neutral, *NC* nonconserved, *NT* nucleotide, *OA* onset age, *PD* probably damaging, *S* sporadic.
[a]The highest subpopulation frequency in the Genome Aggregation Database (gnomAD) is shown.

influence regional conformation (Fig. 2d). Asn590 is located in TM11 (Fig. 2c), and replacement of Asn590 with Ser alters the interhelical hydrogen bonds between Arg593 in TM11 and Gln1239 in TM17, which may influence the stability of the helix–helix structure and change the conformation of the substrate binding pocket (Fig. 2d).

Abcc1 expression in mouse inner ear

To further evaluate the role of *Abcc1* in the auditory system, we analyzed the expression of *Abcc1* in mouse inner ear. RT-PCR showed *Abcc1* was expressed in P3–4 mice inner ear (Fig. 3a). Western blot confirmed the expression of Abcc1 in mice inner ear (Fig. 3b). To investigate the distribution of Abcc1 in mouse cochlea, we performed cryosections of inner ears on P28 mice. Immunoreactivity for Abcc1 was localized on stria vascularis as well as auditory nerves with a cytomembrane distribution (Figs. 3c, d and 4e). Higher-magnification views showed immunostaining for Abcc1 mainly in marginal and intermediate cells of stria vascularis (Fig. 4d), suggesting the protein may function in exchanging substances in the inner ear.

Variant p.Asn590Ser shows deleterious in vitro functional analysis

As shown in Fig. 4a, confocal microscopy shows that WT and p.Asn590Ser variant proteins were both routed to the cytomembrane in no permeabilized HEK cells. When permeabilized by 0.1% TritonX-100, WT protein had a normal distribution, while variant p.Asn590Ser showed expression in both membrane and cytoplasm. To recapitulate the consequences of the hearing loss–associated variant in vivo, we took Epstein–Barr virus–transformed lymphoblastoid cell lines obtained from affected and unaffected siblings in family HN-SD01 as cell models for further functional analysis. Sanger sequencing of total RNA RT-PCR products showed that c.1769A>G was transcribed to mRNA in lymphoblastoid cell lines (Supplementary Figure 1). RT-qPCR analysis demonstrated that the missense variant decreased mRNA expression level of *ABCC1* compared with normal controls (Fig. 4b). Cycloheximide blocks protein synthesis by binding the ribosome and inhibiting eEF2-mediated translocation.[19] Since ribosome association inhibits eukaryotic mRNA degradation, cycloheximide also inhibits mRNA degradation.[20] We used cycloheximide (1:200, MCE, HY-12320) to treat the cell line. RT-qPCR results demonstrated that there was an increasing level of mRNA in cells from affected individuals after being treated with cycloheximide (Fig. 4c), suggesting that this missense variant produced unstable mRNA.

To determine the functional consequence of p.Asn590Ser, we examined the export of SNARF-1, an MRP1-specific substrate.[16] Loss of SNARF-1 in cells is a robust measure of MRP1 efflux activity.[17] In affected lymphoblastoid cells, SNARF-1 was exported more slowly than in unaffected cells at 2 hours (Fig. 4d). By 6 hours, both groups were nearly unloaded with the dye.

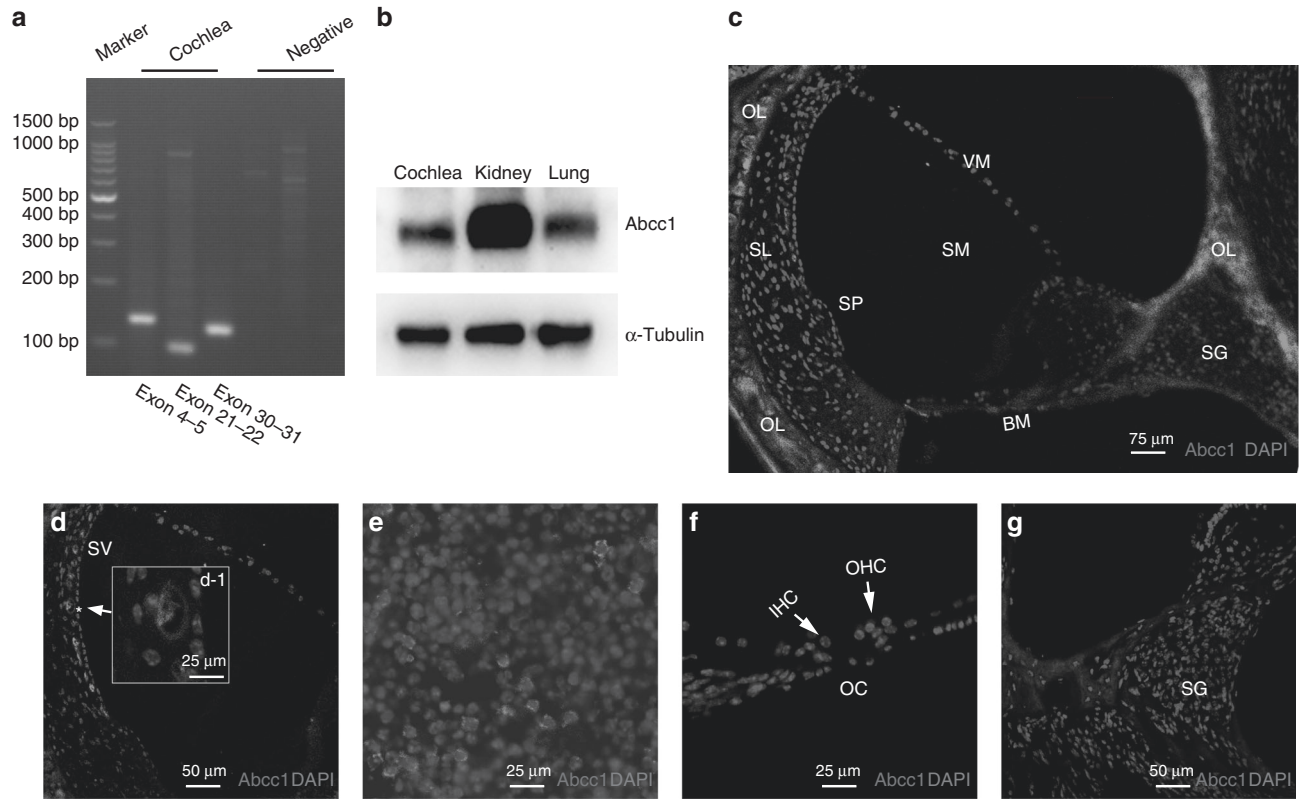

Fig. 3 Expression of *Abcc1* in mouse inner ear. (**a**) Reverse transcription polymerase chain reaction (RT-PCR) analysis of *Abcc1* expression in mouse cochlea. RT products without reverse transcriptase were used as negative controls. (**b**) Expression of Abcc1 was detected in mouse kidney, lung, and cochlea at P3–4. Equal protein loading was confirmed by blotting for α-tubulin. (**c**) Frozen sections of P28 mouse cochlea show Abcc1 (red) distributed in stria vascularis (SV). Sections were counterstained with DAPI (blue) to identify nuclei. (**d**) Abcc1 mainly expressed in marginal and intermediate cells of SV. (**e**) Expression of Abcc1 was detected in mouse auditory nerves. (**f**, **g**) Fluorescence was not found in hair cells and spiral ganglion. *BM* basilar membrane, *IHC* inner hair cells, *OC* organ of Corti, *OHC* outer hair cells, *OL* osseous labyrinth, *SG* spiral ganglion, *SL* spiral ligament, *SM* scala media, *SP* spiral prominence, *VM* vestibular membrane.

DISCUSSION

In this study, we first linked extruding pump *ABCC1* with nonsyndromic hearing loss using stepwise genetic analysis. In brief, gene microarray detection excluded hotspot variant in HN-SD01. High-frequency variants of deafness genes were also excluded in our research. Subsequently, screening for known hearing loss genes was implemented by our virtual hearing loss gene panel. After excluding all known genes, parametric genome-wide linkage analysis was performed to identify the region harboring the novel gene causing the HL in this family. High throughput is a significant advantage of ES, making it capable of providing comprehensive variation data;[21] however, this also makes it difficult for researchers to recognize pathogenic variants from the massive amount of data. To resolve this conflict, we presented the concept of the virtual hearing loss gene panel, an ES-based disease-associated bioinformatic analysis strategy. This panel includes all known hearing loss genes and genes associated with syndromes including hearing loss. This analysis strategy is both time- and cost-effective. Analysis of known hearing loss genes can be easily acquired without additional cost of massively parallel sequencing panels, and genes on the panel can be updated immediately upon the discovery of a new gene for hearing loss. It is also suitable for reanalysis of ES data for detecting unknown hearing loss genes. By stepwise genetic analysis, *ABCC1* (NM_004996.3:c.1769A>G) was finally identified as the only variant segregating with phenotype in HN-SD01.

ABCC1 maps to chromosome 16p13.1 and encodes the 1531–amino acid multidrug resistance protein 1 (MRP1).[4] It belongs to the ABC transporter family and contains five domain structures including two nucleotide binding domains (NBDs) and 17 transmembrane helices (TMs) in three transmembrane domains (TMD0, TMD1, and TMD2).[22] TMD1 and TMD2 are canonical domains and form the substrate translocation pathway. The NH2-terminal TMD0, which is absent in typical ABC proteins, is connected to TMD1 by linker L0 at the COOH-terminus.[23] TM11 is the last helix of TMD1 and predicted to form part of the transporter's substrate binding pocket.[24] A number of polar residues within or near TM11, including Asn590, Arg593, Phe594, Asn597, and Ser604, function in determining the substrate specificity or overall activity of the protein.[24,25] Three-dimensional modeling of MRP1 illustrates that the substitution of the conserved amino acid Asn590 with Ser may change the hydrogen-bonding capacity of the side chain at position 590. Further analysis indicates that the original

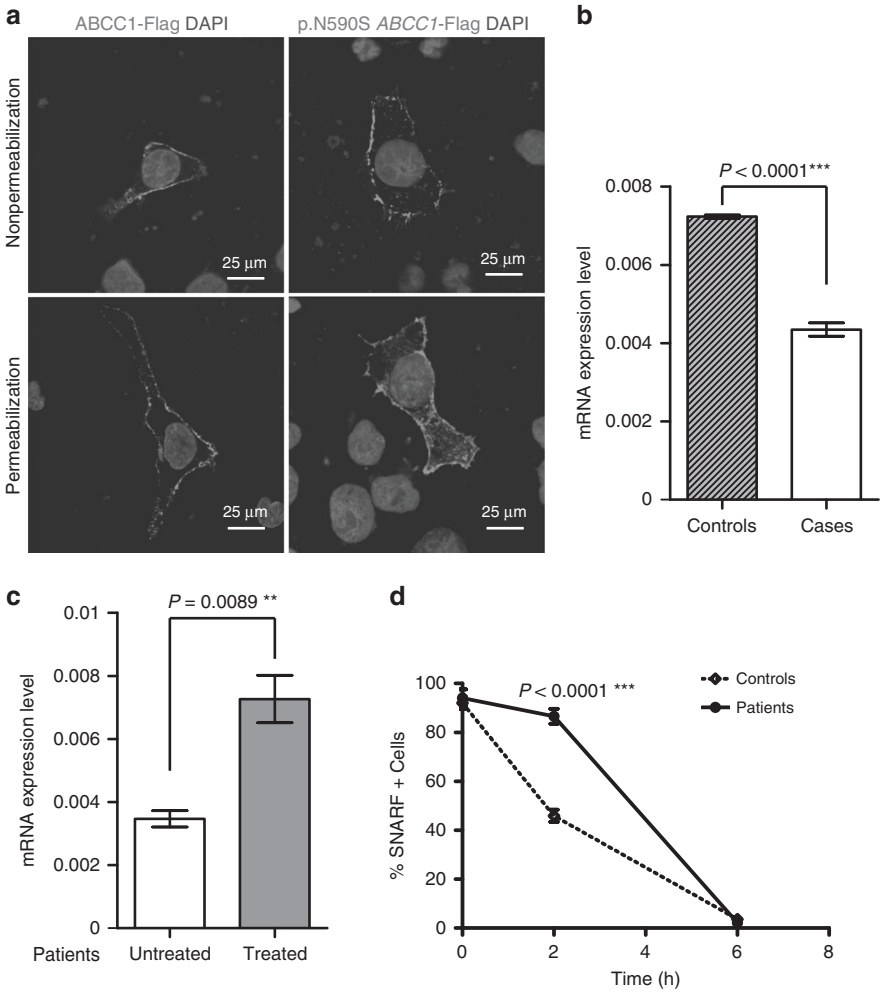

Fig. 4 Functional analysis of variant p.Asn590Ser in vitro. (**a**) When permeabilized by 0.1% TritonX-100, wild type (WT) presented normal distribution, while p.Asn590Ser showed expression in both membrane and cytoplasm. (**b**) Real-time quantitative polymerase chain reaction (RT-qPCR) indicated that the messenger RNA (mRNA) expression level of affected lymphocyte cells decreased compared with unaffected. (**c**) After being treated by cycloheximide, mRNA expressing level of *ABCC1* was increased in affected lymphocytes. (**d**) SNARF-1 efflux assay in affected and unaffected lymphocytes. SNARF-1 was exported more slowly in affected lymphocytes than unaffected at 2 hours. By 6 hours, the two groups were nearly unloaded with the dye.

interhelical hydrogen bonds (Arg593 and Gln1239) between TM11 and TM17 might be altered (Ser590 and Gln1239), which may influence the stability of the helix–helix structure and change the conformation of substrate binding pocket. In vitro functional analysis indicates that p.Asn590Ser might alter the subcellular distribution of MRP1 and cause unstable mRNA. Transport activity measured by the efflux of SNARF-1 was significantly decreased in lymphoblastoid cells from affected individuals. The other two variants, p.Gly231Asp and p.Glu296Val, are both located in the L0 linker, and were identified in sporadic and familial probands, respectively, with postlingual hearing loss. The sequence of L0 is conserved in all 13 members of the ABCC subfamily and forms a structural motif that interacts with the transmembrane region.[26] Deletion of L0 resulted in defective transporters, implying L0 functions in facilitating proper folding and trafficking of MRP1.[27] Converting Gly231 to Asp may alter hydrogen bonds between L0 and TM15, and replacement of Glu296 with Val may change the hydrogen bonds in adjacent amino acids. Consequently, both variants might result in regional conformation changes and interfere with the transport function of the protein.

MRP1 transports a structurally diverse range of endogenous substances (leukotrienes and estrogen conjugates) as well as xenobiotics and their metabolites, including various conjugates, anticancer drugs, heavy metals, organic anions, and lipids. It is ubiquitously expressed in kidney, lung, testes, intestine, and particular cells at the interface between tissues and systemic circulation, such as the blood–brain barrier (BBB) and the choroid plexus of the blood–cerebrospinal fluid barrier.[28] Although MRP1 was originally identified as an alternative multidrug transporter in drug-selected cell lines, it turned out to be a protein with multiple physiological functions, including defense against xenobiotics and endogenous toxic metabolites, leukotriene-mediated inflammatory responses, as well as protection from the toxic effect of oxidative stress.[6,29] *Abcc1*(-/-) mice are usually associated with research on drug resistance, central nervous system disease

(such as Alzheimer disease), chemotherapeutic drug–related cytotoxicity, and so on.[6] However, they have not been investigated for hearing loss. Previous reports showed that people with a 16p13.11 microdeletion including gene *ABCC1* have developmental deficits, exhibiting a common delay in speech and language, abnormal behavior, difficulty in learning, and hearing impairment. Some children with this deletion have permanent sensorineural hearing loss with or without inner ear malformation.[30,31] Takehisa[32] first detected MRP1 expression in rat cochlea including stria vascularis, spiral ligament, spiral prominence, and cochlear nerve in the modiolus. Subsequently, he also confirmed the presence of MRP1 in the vestibular labyrinth and endolymphatic sac of the guinea pig by immunohistochemical staining.[33] Consistent with this research, we also found expression of MRP1 mainly in the stria vascularis and cochlear nerve of mouse inner ear. Stria vascularis is an important component of the blood–inner ear barrier and is associated with transport of selective substances between the blood and endolymph.[34] For the cochlear nerve, there may be also a blood–nerve barrier protecting neurons and fibers against neurotoxic substances. MRP1 may function as a pump to extrude toxic xenobiotics and metabolic waste products from endolymph. Consequently, MRP1 may exhibit a protective role in maintaining the homeostasis of the inner ear. Decline in activity may lead to impairment of inner ear function resulting in late-onset hearing loss.

A limitation of our study is that the individuals were limited to Chinese Han. We will conduct further research in other populations to determine whether variants in *ABCC1* are pan-ethnic. In addition, incomplete capture and coverage are a limitation for the use of ES in genetic diagnosis of hearing loss compared with a specified gene panel. Improvements in capture and enrichment technology will increase the use of ES in clinical diagnosis of hearing loss. In the future, we will perform large-scale research to evaluate the diagnostic efficiency, cost, and turnaround time of a hierarchical genetic analysis strategy based on ES.

In summary, we first associate extrusion pump *ABCC1* with hearing loss in humans using stepwise genetic analysis. Our research suggests that disorder of the extrusion system, especially in stria vascularis, may be an important pathological mechanism for hearing loss. Our data also have implications for future molecular and clinical diagnosis of hearing loss. Further research should be performed to determine the potential contribution of *ABCC1* to hearing loss, which will be beneficial for future treatment strategies.

SUPPLEMENTARY INFORMATION

The online version of this article (https://doi.org/10.1038/s41436-019-0594-y) contains supplementary material, which is available to authorized users.

ACKNOWLEDGEMENTS

The authors greatly thank all the patients and their family members who participated in this study. The research was supported by grants from the National Natural Science Foundation of China (grant numbers 81771023, 81873705, 81771024, and 81700923), the Major State Basic Research Development Program of China (973 Program) (grant number 2014CB541702), the China Postdoctoral Science Foundation (grant numbers 2018M632999, 2017M620359), and the National Institutes of Health/National Institute on Deafness and Other Communication Disorders (grant numbers R01 DC005575 and R01 DC012115).

DISCLOSURE

The authors declare no conflicts of interest.

REFERENCES

1. Morton CC, Nance WE. Newborn hearing screening—a silent revolution. N Engl J Med. 2006;354:2151–2164.
2. Petersen MB. Non-syndromic autosomal-dominant deafness. Clin Genet. 2002;62:1–13.
3. Wang L, Feng Y, Yan D, et al. A dominant variant in the PDE1C gene is associated with nonsyndromic hearing loss. Hum Genet. 2018;137:437–446.
4. Cole SP, Bhardwaj G, Gerlach JH, et al. Overexpression of a transporter gene in a multidrug-resistant human lung cancer cell line. Science. 1992;258:1650–1654.
5. Yin J, Zhang J. Multidrug resistance-associated protein 1 (MRP1/ABCC1) polymorphism: from discovery to clinical application. Zhong Nan Da Xue Xue Bao Yi Xue Ban. 2011;36:927–938.
6. Cole SP. Multidrug resistance protein 1 (MRP1, ABCC1), a "multitasking" ATP-binding cassette (ABC) transporter. J Biol Chem. 2014;289:30880–30888.
7. Semsei AF, Erdelyi DJ, Ungvari I, et al. ABCC1 polymorphisms in anthracycline-induced cardiotoxicity in childhood acute lymphoblastic leukaemia. Cell Biol Int. 2012;36:79–86.
8. Krohn M, Lange C, Hofrichter J, et al. Cerebral amyloid-beta proteostasis is regulated by the membrane transport protein ABCC1 in mice. J Clin Invest. 2011;121:3924–3931.
9. Li W, Sun J, Ling J, et al. ELMOD3, a novel causative gene, associated with human autosomal dominant nonsyndromic and progressive hearing loss. Hum Genet. 2018;137:329–342.
10. Dai P, Yu F, Han B, et al. GJB2 mutation spectrum in 2,063 Chinese patients with nonsyndromic hearing impairment. J Transl Med. 2009;7:26.
11. Hu H, Wu L, Feng Y, et al. Molecular analysis of hearing loss associated with enlarged vestibular aqueduct in the mainland Chinese: a unique SLC26A4 mutation spectrum. J Hum Genet. 2007;52:492–497.
12. Huang S, Han D, Yuan Y, et al. Extremely discrepant mutation spectrum of SLC26A4 between Chinese patients with isolated Mondini deformity and enlarged vestibular aqueduct. J Transl Med. 2011;9:167.
13. Li Z, Li R, Chen J, et al. Mutational analysis of the mitochondrial 12S rRNA gene in Chinese pediatric subjects with aminoglycoside-induced and nonsyndromic hearing loss. Hum Genet. 2005;117:9–15.
14. Oza AM, DiStefano MT, Hemphill SE, et al. Expert specification of the ACMG/AMP variant interpretation guidelines for genetic hearing loss. Hum Mutat. 2018;39:1593–1613.
15. Zhang H, Chen H, Luo H, et al. Functional analysis of Waardenburg syndrome-associated PAX3 and SOX10 mutations: report of a dominant-negative SOX10 mutation in Waardenburg syndrome type II. Hum Genet. 2012;131:491–503.
16. Jin J, Jones AT. The pH sensitive probe 5-(and-6)-carboxyl seminaphthorhodafluor is a substrate for the multidrug resistance-related protein MRP1. Int J Cancer. 2009;124:233–238.
17. Weekes MP, Tan SY, Poole E, et al. Latency-associated degradation of the MRP1 drug transporter during latent human cytomegalovirus infection. Science. 2013;340:199–202.
18. Richards S, Aziz N, Bale S, et al. Standards and guidelines for the interpretation of sequence variants: a joint consensus recommendation

of the American College of Medical Genetics and Genomics and the Association for Molecular Pathology. Genet Med. 2015;17:405–424.
19. Schneider-Poetsch T, Ju J, Eyler DE, et al. Inhibition of eukaryotic translation elongation by cycloheximide and lactimidomycin. Nat Chem Biol. 2010;6:209–217.
20. Roy B, Jacobson A. The intimate relationships of mRNA decay and translation. Trends Genet. 2013;29:691–699.
21. Atik T, Bademci G, Diaz-Horta O, et al. Whole-exome sequencing and its impact in hereditary hearing loss. Genet Res (Camb). 2015;97:e4.
22. Varadi A, Tusnady GE, Bakos E, Sarkadi B. Membrane topology of the human multidrug resistance-associated protein (MRP) and its homologs. Cytotechnology. 1998;27:71–79.
23. Bakos E, Evers R, Calenda G, et al. Characterization of the amino-terminal regions in the human multidrug resistance protein (MRP1). J Cell Sci. 2000;113 Pt 24:4451–4461.
24. Zhang DW, Nunoya K, Vasa M, et al. Transmembrane helix 11 of multidrug resistance protein 1 (MRP1/ABCC1): identification of polar amino acids important for substrate specificity and binding of ATP at nucleotide binding domain 1. Biochemistry. 2004;43:9413–9425.
25. Koike K, Conseil G, Leslie EM, et al. Identification of proline residues in the core cytoplasmic and transmembrane regions of multidrug resistance protein 1 (MRP1/ABCC1) important for transport function, substrate specificity, and nucleotide interactions. J Biol Chem. 2004;279:12325–12336.
26. Johnson ZL, Chen J. Structural basis of substrate recognition by the multidrug resistance protein MRP1. Cell. 2017;168:1075–1085.
27. Bakos E, Evers R, Szakacs G, et al. Functional multidrug resistance protein (MRP1) lacking the N-terminal transmembrane domain. J Biol Chem. 1998;273:32167–32175.
28. Cartwright TA, Campos CR, Cannon RE, Miller DS. Mrp1 is essential for sphingolipid signaling to p-glycoprotein in mouse blood-brain and blood-spinal cord barriers. J Cereb Blood Flow Metab. 2013; 33:381–388.
29. Cole SP. Targeting multidrug resistance protein 1 (MRP1, ABCC1): past, present, and future. Annu Rev Pharmacol Toxicol. 2014; 54:95–117.
30. Nagamani SC, Erez A, Bader P, et al. Phenotypic manifestations of copy number variation in chromosome 16p13.11. Eur J Hum Genet. 2011; 19:280–286.
31. Hannes FD, Sharp AJ, Mefford HC, et al. Recurrent reciprocal deletions and duplications of 16p13.11: the deletion is a risk factor for MR/MCA while the duplication may be a rare benign variant. J Med Genet. 2009;46:223–232.
32. Saito T, Zhang ZJ, Tokuriki M, et al. Expression of multidrug resistance protein 1 (MRP1) in the rat cochlea with special reference to the blood-inner ear barrier. Brain Res. 2001;895:253–257.
33. Saito T, Zhang ZJ, Tokuriki M, et al. Expression of p-glycoprotein is associated with that of multidrug resistance protein 1 (MRP1) in the vestibular labyrinth and endolymphatic sac of the guinea pig. Neurosci Lett. 2001;303:189–192.
34. Shi X. Pathophysiology of the cochlear intrastrial fluid-blood barrier (review). Hear Res. 2016;338:52–63.